Development of Polyurethane Engineering Thermoplastics. I. Preparation and Structure

PATRICIA M. FRONTINI,* MARTA RINK, and ANDREA PAVAN

Dipartimento di Chimica Industriale e Ingegneria Chimica, Politecnico di Milano, Piazza L. da Vinci 32, 20133 Milano, Italy

SYNOPSIS

Rigid, tough thermoplastic copolyurethanes were prepared by a prepolymer technique. The soft-segment content was varied over the 5–30 wt %. Six stoichiometric formulations based on diphenylmethane 4,4′-diisocyanate (MDI), one or two different polyetherglycols, and one or two chain extenders of different structure were examined to test the possibilities of varying the degree of crystallinity of the products. Despite their thermoplastic characteristics, the resulting products were insoluble in the solvents normally used for elastomeric polyurethanes. The influence of curing temperature upon crystallinity and degree of polymerization was analyzed. Phase-structure analysis, performed by differential scanning calorimetry, dynamic-mechanical thermal analysis, and wide-angle X-ray scattering revealed complex phase structures strongly dependent on previous thermal history. In any case, the soft segments appear to constitute a dispersed phase in a rigid amorphous or semicrystalline matrix. Some samples exhibited two hard-segment glass transitions associated with the existence of a bimodal length hard-segment distribution. X-ray diffraction patterns suggested that more than one crystalline form was present in the crystalline phase. © 1993 John Wiley & Sons, Inc.

1. INTRODUCTION

Linear segmented polyurethane elastomers have developed greatly, since they are easy to process and have appealing physical and mechanical properties. Polyether and polyester linear urethane systems were first described by Bonart[1] as consisting of "hard" and "soft" segments, with the "hard" segments acting as "physical cross-links." Considerable research effort has been directed toward understanding properties,[2] macro- and microphase separation,[3–8] and the structure and morphology of the crystalline hard domains[9–11] in diphenylmethane 4,4′-diisocyanate (MDI)/diol-based segmented polyurethane elastomers. The influence of physical variables,[12] chemical composition,[13] and polymerization techniques[14,15] on final properties has also been discussed.

Rigid thermoplastic copolyurethanes, on which the information available in the literature is scarce, have received less attention.[16–18] They are multiphase systems comprising soft domains dispersed within a hard matrix. The present work was aimed at gaining a deeper insight into the structure-to-properties relationships of rigid thermoplastic copolyurethanes.

By varying composition, conditions of bulk polymerization, and processing (molding and post-molding thermal treatments), we attempted to obtain polyurethanes with high softening temperature and toughness, which could compete with other engineering thermoplastics while preserving the advantages of polyurethanes such as chemical inertia and ease of manufacture.

This research work falls into two parts: The first (reported in the present paper) discusses the influence of formulation, polymerization conditions, and thermal treatments on the degree of polymerization and phase structure of the resulting products. The second (to be published subsequently) deals with mechanical characterization of these new materials

* To whom correspondence should be addressed at Institute of Materials Science and Technology (INTEMA), J.B. Justo 4302. 7600, Mar del Plata, Argentina.

Journal of Applied Polymer Science, Vol. 48, 2003–2022 (1993)
 CCC 0021-8995/93/112003-20

and aims to correlate their mechanical properties with crystallinity and the hard/soft segment ratio.

2. EXPERIMENTAL

2.1. Reagents and Formulations

The polyurethanes studied are multicomponent systems based on a diisocyanate, one or two different polyether polyols, and one or two chain extenders. The following chemicals were used:

Diisocyanate:

- Frozen diphenylmethane 4,4′-diisocyanate (MDI) (Montedipe, Italy) was melted and then stocked, in the liquid state, at 42°C to avoid dimerization. Only the clear supernatant was used.

Polyols:

- Polypropylene oxide diol (DIOL) (Montedipe, Italy) with hydroxyl number 55, M_w = 2000, and T_g = −70°C.
- Polypropylene oxide endcapped with ethylene oxide (TRIOL) (Montedipe, Italy) with hydroxyl number 34 and M_w = 5000.

Chain extenders:

- 1,4-Butanediol (BDO) (Aldrich, U.S.A.).
- Diethylene glycol (DEG) (Carlo Erba, Italy).
- Triethylene glycol (TEG) (Carlo Erba, Italy).
- 2-Ethyl-2-methyl-1,3-propanediol (EMPDO) (Fluka, Switzerland).
- 1-Phenyl-1,2-ethanediol (PhEDO) (Aldrich, U.S.A.).

All glycols were dried and degassed under vacuum up to a residual water content of less than 300 ppm.

Table I shows the six stoichiometric types of polyurethane materials investigated here. Each type was examined at several hard/soft ratios. The hard-segment and soft-segment contents are defined as a percentage by weight of the isocyanate and chain extenders and as a percentage by weight of the polyols, respectively. Each sample was labeled with a three-sequence code, indicating, respectively, the hard/soft segment ratio, the polyurethane type (as indicated in Table I), and the curing temperature used. For instance, 80/20 : I : 120 means that the

Table I Description of Polyurethanes Synthetized

Type	Components	Molar Ratio between Chain Extenders	Mass Ratio between Polyols	$\frac{\text{Equiv}_{NCO}}{\text{Equiv}_{OH}}$
I	BDO MDI DIOL	—	—	1
II	BDO–DEG MDI DIOL–TRIOL	$\frac{N_{BDO}}{N_{DEG}} = \frac{4}{1}$	$\frac{m_{DIOL}}{m_{TRIOL}} = \frac{1}{1}$	1
III	BDO–DEG MDI DIOL–TRIOL	$\frac{N_{BDO}}{N_{DEG}} = \frac{1}{1}$	$\frac{m_{DIOL}}{m_{TRIOL}} = \frac{1}{1}$	1
IV	BDO–TEG MDI DIOL–TRIOL	$\frac{N_{BDO}}{N_{TEG}} = \frac{4}{1}$	$\frac{m_{DIOL}}{m_{TRIOL}} = \frac{1}{1}$	1
V	BDO–EMPDO MDI DIOL–TRIOL	$\frac{N_{BDO}}{N_{EMPDO}} = \frac{4}{1}$	$\frac{m_{DIOL}}{m_{TRIOL}} = \frac{1}{1}$	1
VI	BDO–PhEDO MDI DIOL–TRIOL	$\frac{N_{BDO}}{N_{PhEDO}} = \frac{4}{1}$	$\frac{m_{DIOL}}{m_{TRIOL}} = \frac{1}{1}$	1

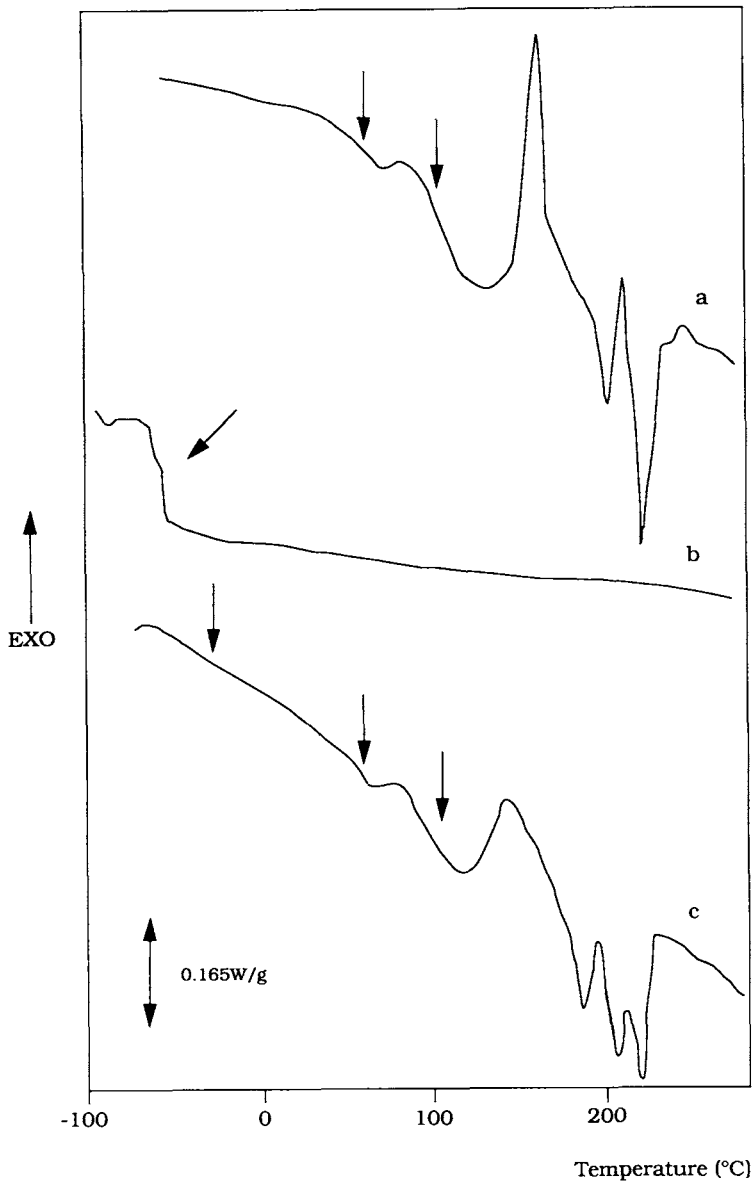

Figure 1 DSC standard scans of samples: (a) 100/0 : I : 110; (b) 0/100 : I : 110; (c) 90/10 : I : 110. Arrows indicate second-order transitions.

sample is a Type I polyurethane, was prepared with a 20% soft-segment content, and was cured at 120°C.

2.2. Polymerization

Batch polymerization was carried out in a 1000 mL stainless-steel stirred reaction vessel, at 80°C, under atmospheric pressure, with a two-step technique (prepolymer method). The two-step method was chosen to ensure the reaction of the secondary hydroxyl groups of the polyol without using a catalyst.

First, a prepolymer made from the polyether glycols and a known excess of MDI was prepared. After the reaction had attained complete conversion (1 h), the appropriate amount of chain extenders (preheated at 80°C) was added, and the mixture was rapidly stirred for about 40 s, poured into a preheated mold, and left to cure in an oven for 15 min, after which it was cooled to ambient temperature.

Before the addition of the chain extenders, 0.5% by weight of an antioxidant (Irganox 1010, Ciba Geigy) was added. The absence of nonreacted isocyanate groups in the products was verified by infrared spectroscopy (absorption band of free NCO group at 2240–2270 cm^{-1} [Ref. 19]).

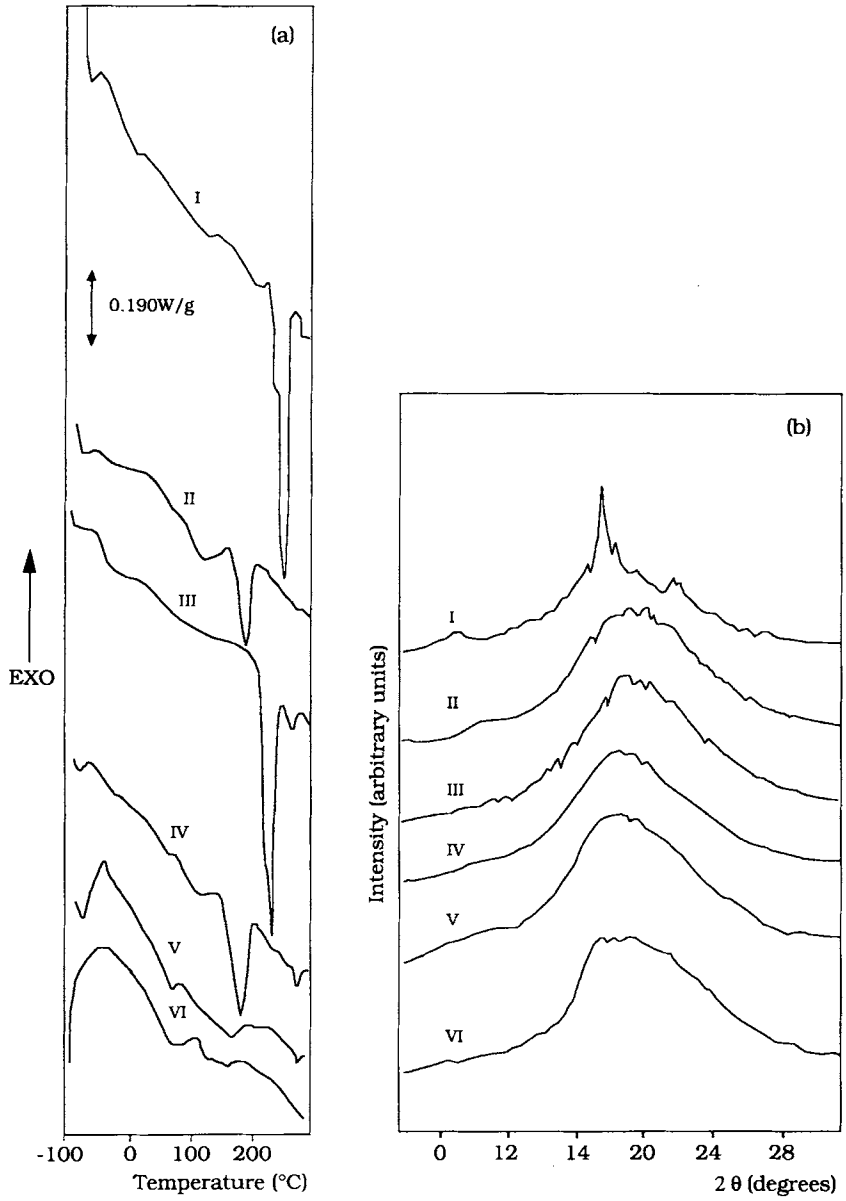

Figure 2 (a) DSC standard scan and (b) WAXS patterns of six polyurethanes having different chain extenders (hard/soft segment ratio 80/20).

2.3. Analytical Techniques

2.3.1. Differential Scanning Calorimetry (DSC)

Thermal characterization was carried out on a Mettler TA 3000 system equipped with a DSC-30 low-temperature module. Temperature calibration was done with a multiple indium–lead–nickel standard. An indium standard was used for heat-flow calibration.

Generally, scans were conducted at a heating rate of 20°C/min from −150 or −100 to 300°C. These conditions will henceforth be called the "standard scan." Other scanning conditions will be specified.

Glass transition temperatures were taken at the inflection points of the thermograms; multiple endotherms were observed, the peak temperatures were taken as melting points, and the heat of fusion was determined by measuring the areas under the melting peaks.

2.3.2. Dynamic Mechanical Thermal Analysis (DMTA)

Measurements were carried out on compression-molded specimens using a dynamic mechanical thermal analyzer by Polymer Laboratories at a fixed

Table II DSC Data for Polyurethanes 90/10 : I and 80/20 : II Prepared at Different Curing Temperatures

Polyurethane Type	Hard/Soft	Curing Temperature (°C)	T_s (°C)	T_i (°C)	T_h (°C)	ΔH_m (J/g)	T_m (°C)
I	90/10	80	—	—	95	27	200
		110	—	50	95	36	218
		135	—	50	—	52	227
		160	—	50	100	44	240
		180	—	50	105	~ 0	—
		220	—	50	105	~ 0	—
II	80/20	110	−50	50	95	8	185
		150	−50	55	—	22	195
		220	−40	50	102	6.9	213
		250	−50	47	100	~ 0	—

frequency of 3 Hz and operating in a double-cantilever bending mode. The temperature range investigated was −150 to 300°C and the sample was scanned at a rate of 3°C/min.

2.3.3. Thermogravimetric Analysis (TGA)

Measurements were carried out using a thermogravimetric Mettler TA 12 analyzer equipped with a differential thermal analyzer module (DTA).

2.3.4. Infrared Analysis (IR)

Infrared spectra (4000–400 cm^{-1}) were obtained with a Perkin-Elmer 1710 infrared Fourier transform spectrometer. Data were taken using KBr pellets for solid samples and between ClNa glasses for liquid samples.

2.3.5. Wide-Angle X-ray Scattering (WAXS)

Wide-angle X-ray scattering studies were performed on a Philips PW 1050 diffractometer employing nickel-filtered CuKα radiation in the reflectance mode. The scan rate of the 2Θ was 2°/min. Tests were carried out on 3.5 mm-thick compression-molded platelets. For quantitative purposes, data were normalized by background noise. The amorphous index was calculated as the relative area of the amorphous region.[20] An amorphous standard template was defined as the pattern of the material that appears markedly amorphous in WAXS, coinciding with DSC thermograms showing no melting.

3. RESULTS AND DISCUSSION

3.1. Solubility

The availability of a solvent is essential for the molecular characterization of thermoplastic polymers by means of standard solution techniques. We tried to dissolve our polyurethanes in dimethyl sulfoxide, a mixture of *o*-cresol and *p*-cresol, formic acid, sulfuric acid, tetrahydrofuran, acetonitrile, *n*-propanol, and methylene iodine, at room temperature without success, even if other authors could do so on products similar to ours, though with higher soft-segment contents.[12,15,21,22]

Dimethylformamide (DMF), hexamethylenephosphoramide, and dimethylacetamide did swell our samples at room temperature, but did not dissolve them completely, even after a long time. The same behavior was observed for all polyurethane types independently of the TRIOL presence (even in this case, the average polyol functionality was less than 2.014). On the other hand, these polymers exhibited high crystallinity levels (see Section 3.3) and, like typical thermoplastics were capable of being molded by applying pressure and heat.

The insolubility of these polymers may, thus, be interpreted in two ways:

(a) By the presence of very few cross-linking sites resulting from cross-link byproducts like allophanates, whose formation is reversible with temperature,[23,24] formed during polymerization, leading to still crystallizable and thermoplasticlike processable materials. However, IR analysis showed that the allo-

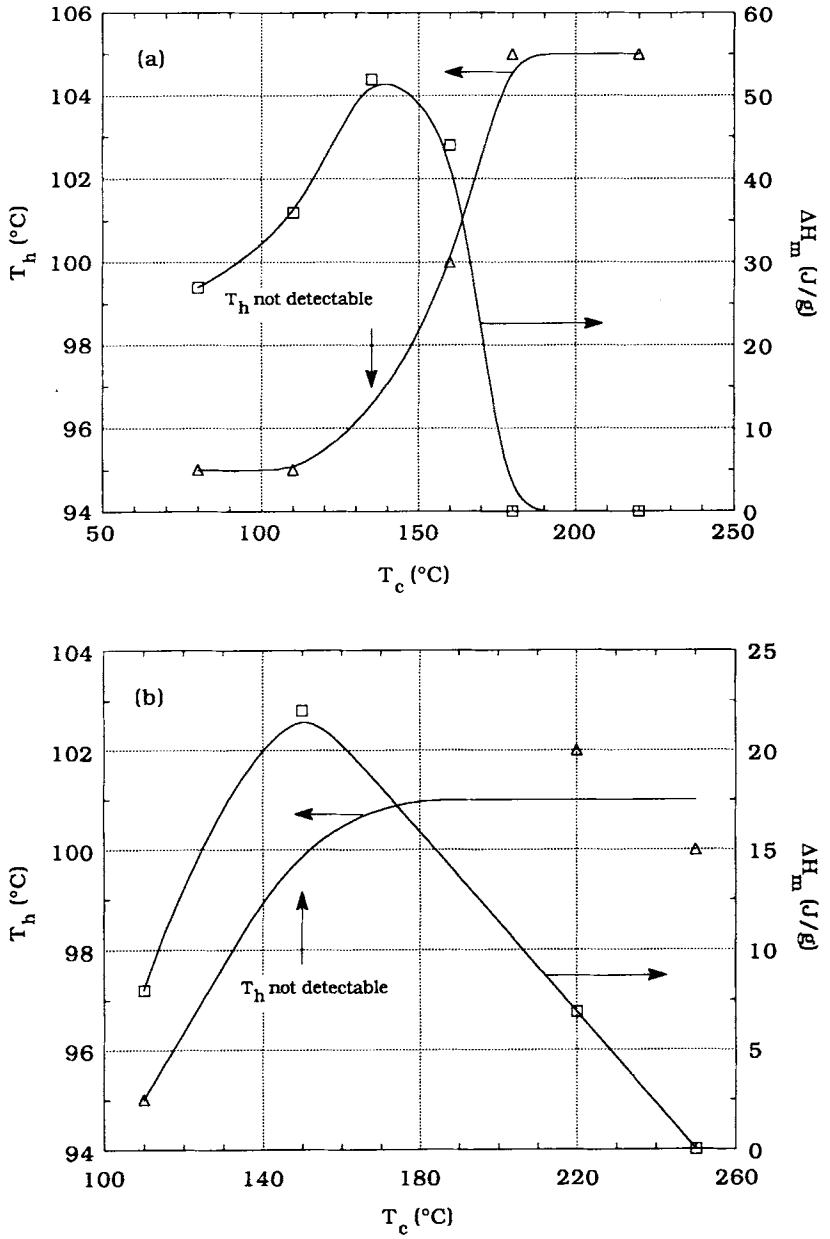

Figure 3 Hard-phase transition temperature, T_h, and heat of fusion, ΔH, as a function of curing temperature for (a) 90/10 : I polyurethanes and (b) 80/20 : II polyurethanes.

phanate absorption band at 1708–1653 cm^{-1} (Ref. 19) was not present. Therefore, if this explanation is valid, allophanate concentration should be below the detection limit of IR measurements.

(b) By the formation of "virtual cross-links" due to the strong hydrogen bonding[25] that can be expected in polyurethanes having such a high hard-segment content, particularly inside crystalline domains.[26]

Since these "virtual cross-links" are reversible[22] with temperature, an increase in solubility could be expected by heating the "dispersions." Dissolution experiments carried out on an 80/20 : II : 250 polyurethane in hot DMF consisting of measuring viscosity at different times, after the complete dissolution of the sample, showed that some degradation occurred simultaneously with dissolution at high temperatures since viscosity decayed constantly during the test. The insolubility of these polymers

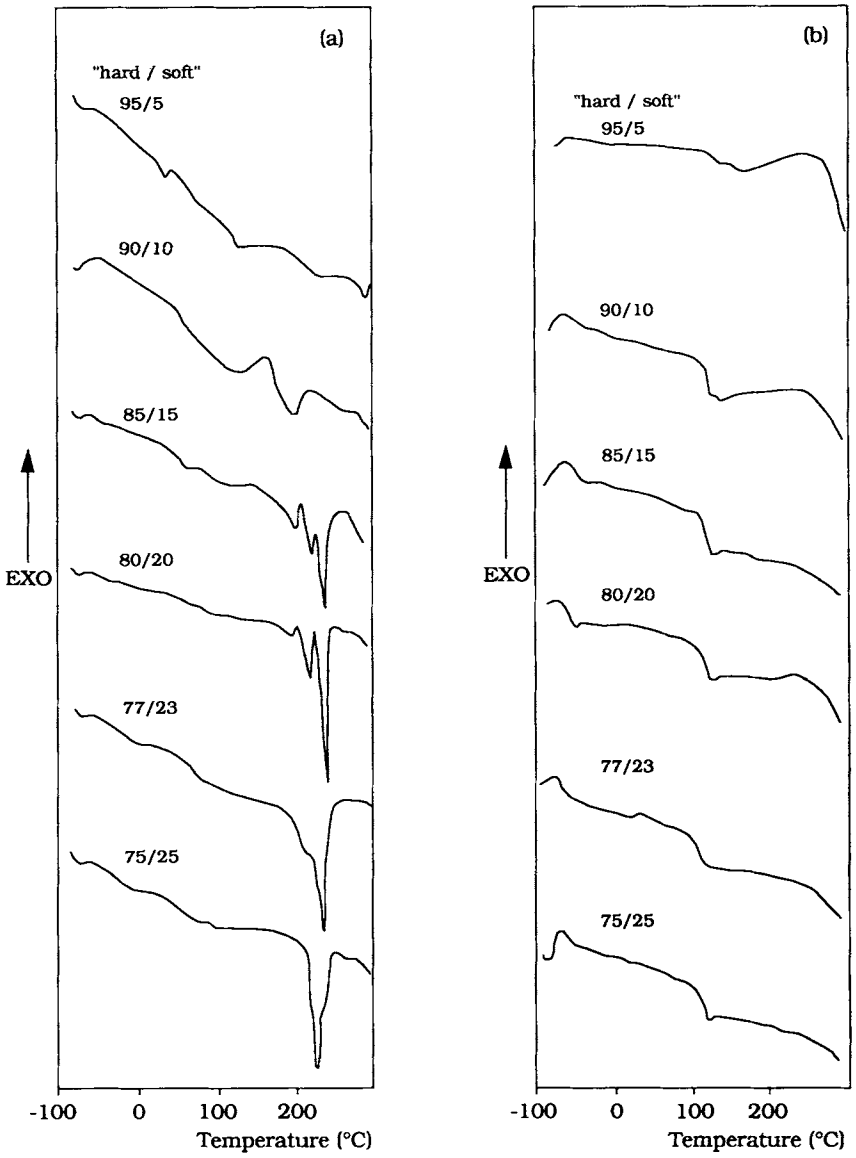

Figure 4 DSC standard scan of Type I polyurethanes at different hard/soft segment ratios (a) after polymerization and (b) after taking the samples to 290°C and cooling them at 5°C/min (thermal treatment "A").

at room temperature may be due to N—H · · · O intermolecular hydrogen bonding generated inside the hard domains. Nevertheless, when solubilization at higher temperatures was capable of destroying the hydrogen bonding, chemical decomposition of the macromolecules also occurred.

3.2. Interpretation of DSC Measurements

Urethane polymers and copolymers are typically characterized by multiphase structures whose organization is related both to the polymer's chemical composition and to the physical treatments that the materials have undergone. For insight into the phase structure of the products obtained, we made use of DSC analysis, which reveals thermal transitions and thus provides some evidence of the phases present. Assignment of the transitions observed to specific phases is not always easy; however, preliminary tests on simpler or "model" systems are often helpful. We thus prepared urethane polymers made of 100% hard segments and 100% soft segments, as well as copolymers with intermediate hard/soft ratios. As an example, Figure 1 shows typical DSC thermo-

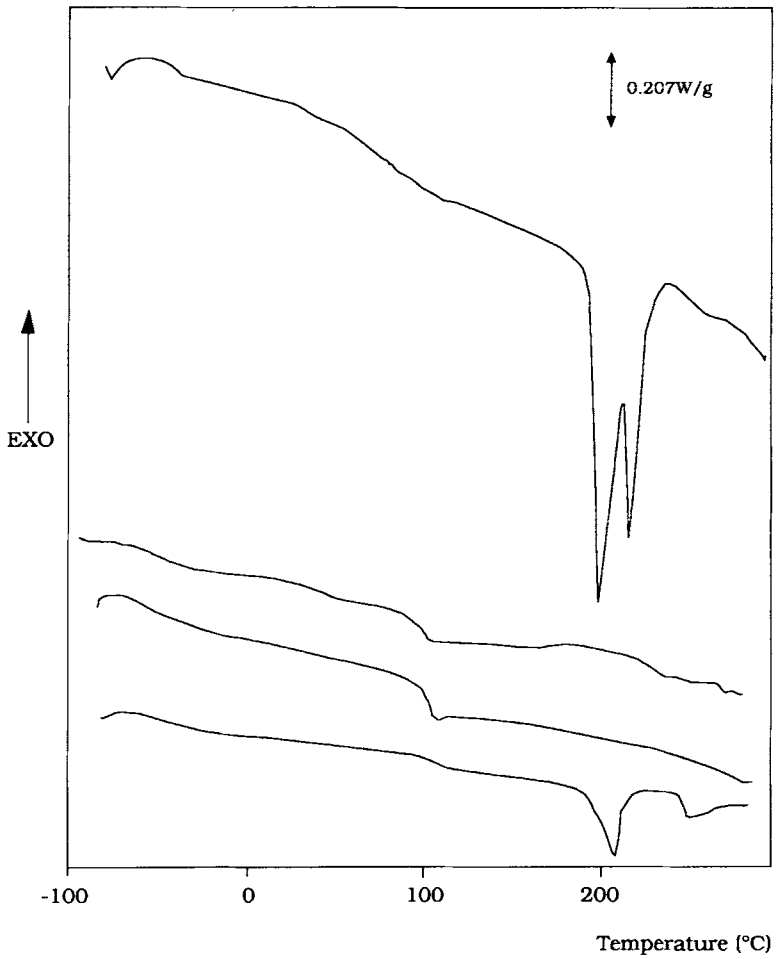

Figure 5 DSC standard scan for the same 80/20 : II : 250 polyurethane showing up four different phase structures.

grams displayed by the 100% hard-segment polymer (obtained from the reaction of MDI with BDO), the 100% soft-segment polymer (obtained from the reaction between MDI with DIOL), and the copolymer 90/10 : I : 110.

For the 100% hard-segment polyurethane, two second-order transitions of the same order of magnitude, at about 50 and 100°C, an exothermic peak at 150°C, and two endothermic peaks at 195 and 220°C are observed. The 100% soft-segment polyurethane shows just one second-order transition at −50°C. This thermogram shows no exo- or endothermal peaks, though sometimes small endothermic peaks were observed with other 100% soft preparations.

As for the copolymer, the second-order transitions at about −50, 50, and 100°C (denoted in the following as T_s, T_i, and T_h, respectively), an exothermic peak at 150°C, and three endothermic peaks between 190 and 235°C are observed. This type of behavior was found for most of the preparations examined.

We thus associated the transition T_s and T_h to the glass transition of the soft and hard segments, respectively, while the nature of the intermediate transition T_i, which seems to be associated to the hard phase, will be discussed later. Phase separation in the amorphous phase, giving rise to two glass transitions such as T_s and T_h, is typical of polyether-based polyurethanes.[1] The exothermic peaks were attributed to crystallization during heating in the calorimeter, since this can take place very fast.[27]

The presence of multiple endothermic peaks, which has also been previously reported by other authors,[8–12,27,28] is associated with the melting of the crystalline phases. The exact position of T_s, T_i, and T_h and the presence, or absence, of endo- and exothermic peaks and their positions depend on the formulation and polymerization conditions used.

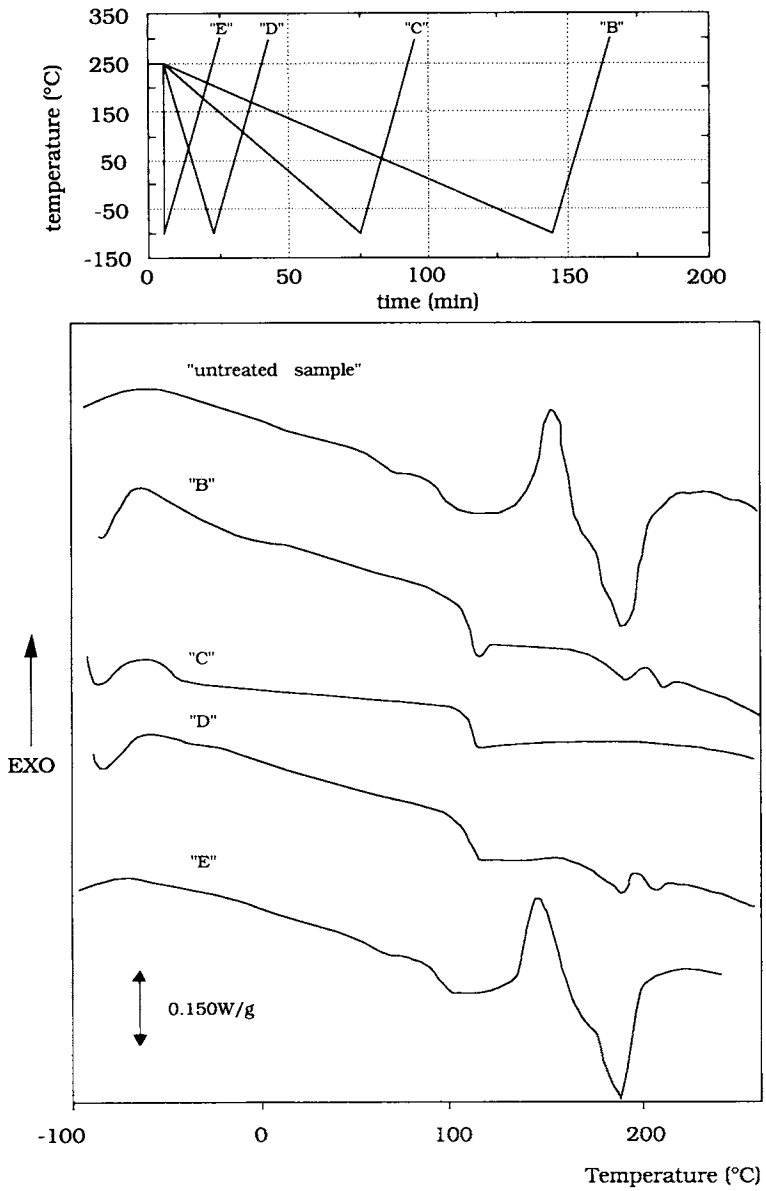

Figure 6 DSC standard scan of an 80/20 : II : 250 polyurethane subjected to four different thermal histories ("B," "C," "D," and "E," respectively).

3.3. Crystallinity and Chain Extenders

The ease of crystallization of the hard segments [Fig. 1, curve (a)] is due to the high degree of symmetry of the MDI molecule. For the purpose of comparing final properties of amorphous and crystalline products, we tried to hinder the hard-phase crystallization. Type I polyurethane was modified by using a mixture of chain extenders of different molecular structure (Types II–VI polyurethanes). All samples were prepared in the same way, with a hard-to-soft ratio of 80/20 and cured at 110°C. Formulations based on polyurethanes Types I–IV show a melting peak in the 170–230°C range in the DSC thermograms [Fig. 2(a)], whereas only sample I displayed distinct crystalline peaks when analyzed by WAXS [Fig. 2(b)].

These apparently contradictory results obtained for samples of Types II–IV can be explained in two ways: either (a) their crystallinity developed during preparation, but the crystals formed are so small and/or imperfect as not to show up under WAXS, though still detectable by DSC; or (b) their crystallinity developed during the temperature scan in

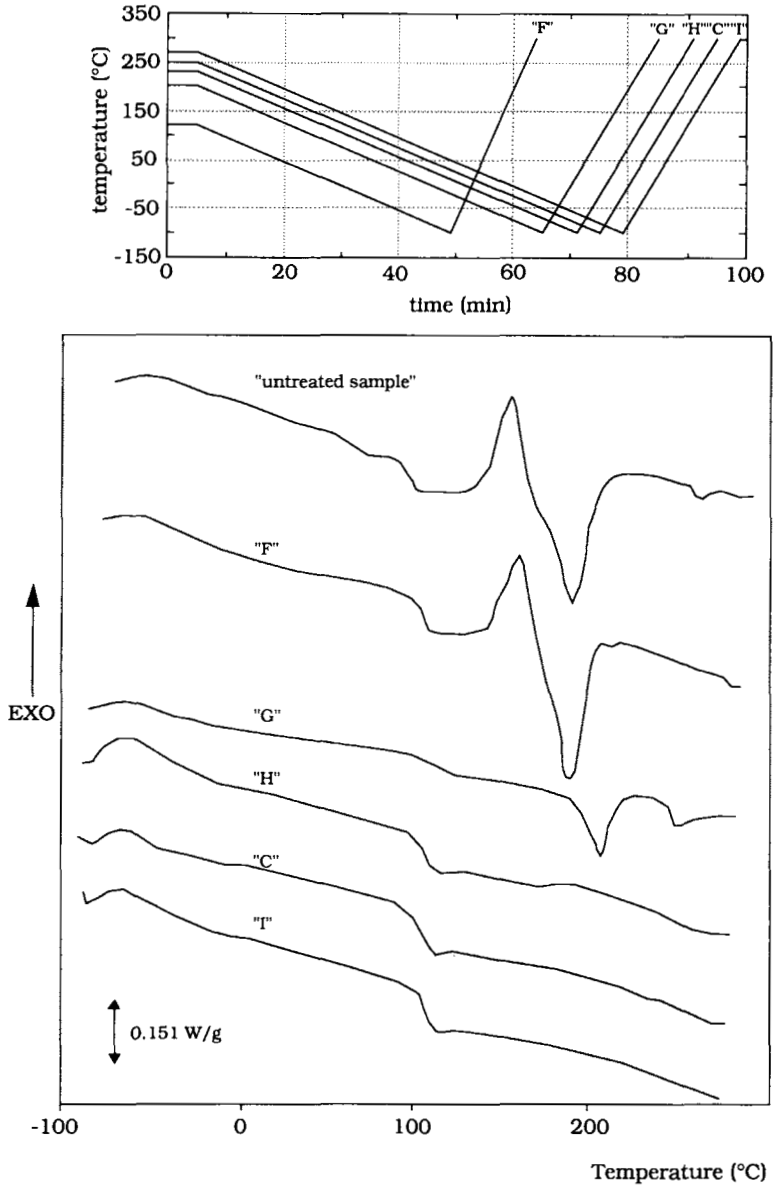

Figure 7 DSC standard scans of 80/20 : II : 250 polyurethane subjected to five different thermal histories ("F," "G," "H," "C," and "I").

the DSC test. Polyurethanes V and VI, instead, turned out to be amorphous under the same polymerization conditions.

3.4. Crystallinity and Curing Temperature

Several Types I and II polyurethanes, both of which had exhibited an appreciable tendency to crystallize, were prepared following the polymerization procedure described in the Experimental section, but with different curing temperatures. Results from DSC analysis are shown in Table II and Figure 3, where the amount of crystallinity (expressed by the heat of fusion ΔH_m), and the glass transition temperature of the hard phase, T_h, are given as a function of curing temperature. It may be observed that similar trends are found for both formulations. Crystallinity as a function of curing temperature displays a maximum at a certain temperature, after which it becomes negligible, thus indicating that amorphous products are obtained for the higher curing temperatures. The glass transition, T_h, increases with curing temperature, reaching asymptotic values, indicating that a maximum degree of polymerization had

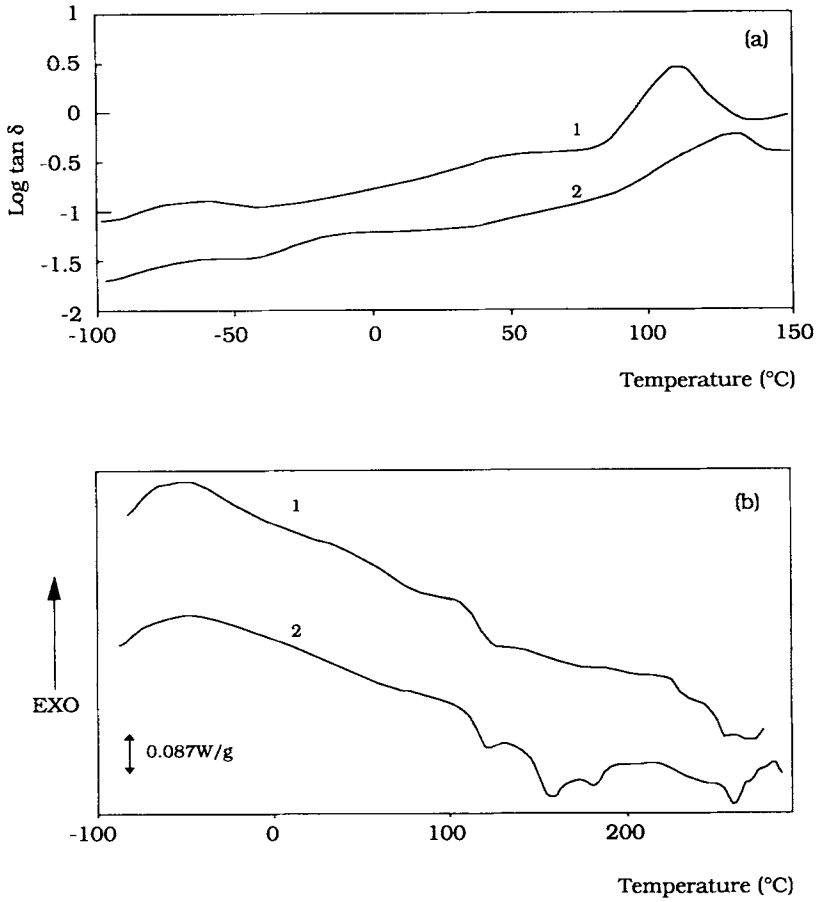

Figure 8 (a) Dynamic mechanical behavior of an 80/20 : VI polyurethane (curve 1). The same material after being kept 5 h at 120°C and then cooled to room temperature at 10°C/min (curve 2). (b) DSC standard scan of an 80/20 : VI polyurethane (curve 1). The same material after being kept 5 h at 120°C and then cooled to room temperature at 10°C/min (curve 2).

been reached; this occurs at the temperatures at which amorphous products are obtained. It is to be noted that these temperatures are well above T_h, indicating that vitrification is not the sole mechanism that can hinder the polymerization. In fact, as has been previously shown,[12] premature crystallization and subsequent phase separation can hamper molecular chain growth.

Some further observations on the results given in Table II are that the soft-phase glass transition, T_s, and the intermediate one, T_i, do not seem to change systematically with curing temperature. Melting temperature, T_m, increases with curing temperature, reaching a maximum value at about 160 and 220°C, respectively, for the two formulations, thus showing that the most ordered structures develop at these temperatures.

3.5. Phase Structure and Thermal Treatments

The phase structure of these materials appears to be strongly affected by the thermal treatment given to the sample. This is clearly shown by a series of six Type I polyurethanes with different hard-to-soft-segment ratios, which were prepared and then subjected to a thermal history (named "A") consisting of heating the sample at a constant heating rate of 20°C/min from room temperature up to 290°C so as to destroy existing crystallinity, and then cooling it down to −100°C at a constant rate of −5°C/min. The "standard DSC scan" of the materials before and after being thermally treated are shown in Figure 4. Irrespectively of the state of the material after polymerization (amorphous or crystalline, with two or three transitions), all the thermally treated sam-

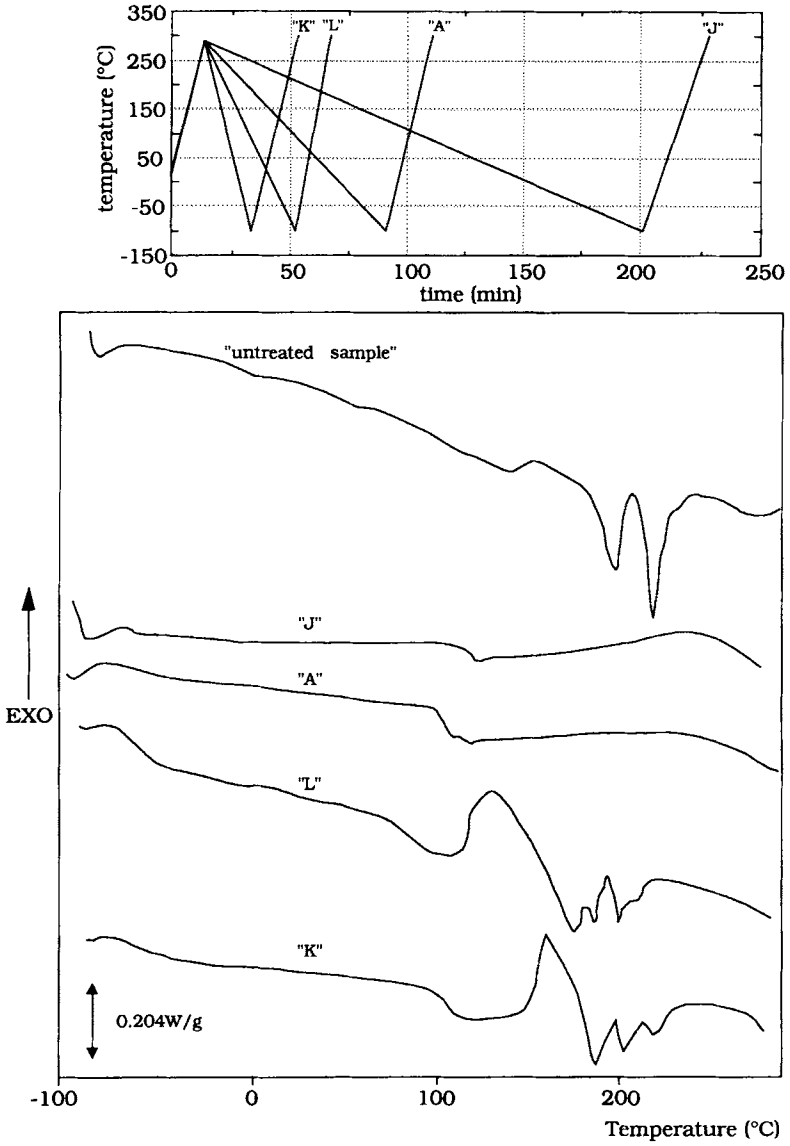

Figure 9 DSC standard scan of 90/10 : I : 110 polyurethane subjected to thermal histories "J," "A," "L," and "K" (also outlined at the top of the figure).

ples show similar phase structure: They are completely amorphous and show only two glass transitions, T_s and T_h. Therefore, this part of our investigation was directed toward understanding the phase behavior and the nature of the thermal transitions observed on samples subjected to various thermal histories.

3.5.1. Analysis of the Influence of Thermal Treatments on the Amorphous Phase

The most significant fact observed in the amorphous phase was the presence or absence of the intermediate transition. Other investigators have previously reported transitions of this type in others polyurethanes,[8,22,29-31] giving different interpretations: Xu et al.,[22] Bengston et al.,[32] and Brunette et al.[29] suggested a bimodal distribution of hard-segment lengths; Curvé et al.[30] suggested a mixed interfacial region; while Lunardon et al.[31] gave two possible interpretations: a β transition or a T_g of a mixed phase. On the basis of our results, the idea of a mixed phase or a mixed interfacial region can be ruled out since the 100% hard material also displays this transition [Fig. 1(a)]. On the other hand, T_i did not exhibit behavior typical of a secondary transition: Such

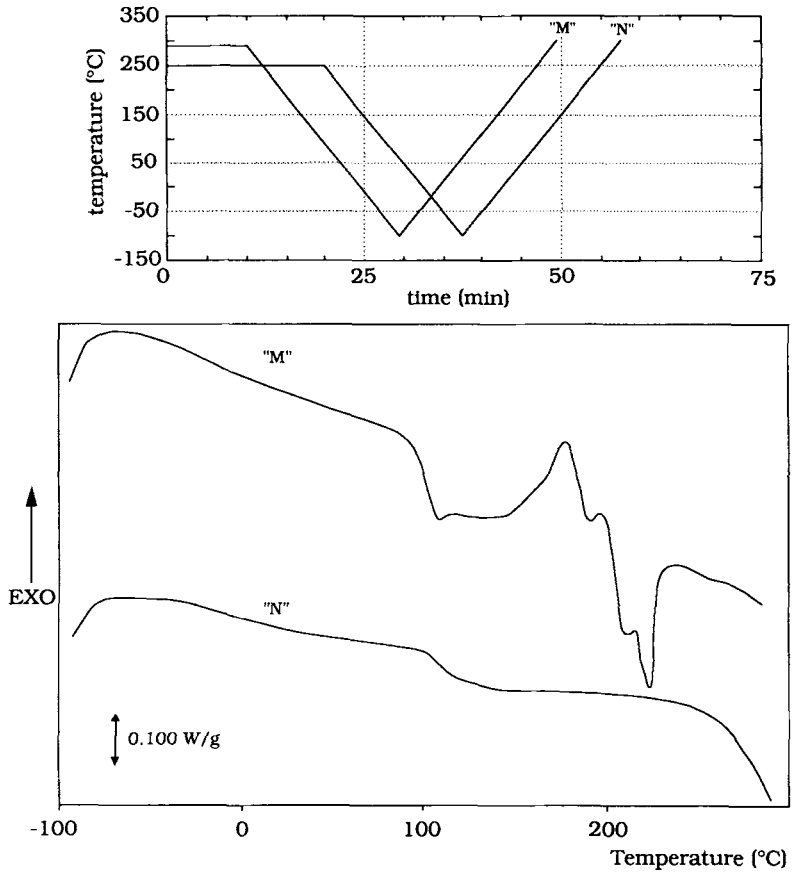

Figure 10 DSC standard scan of 90/10 : I : 110 polyurethane subjected to thermal histories "M" and "N" (also outlined at the top of the figure).

transitions are usually not detectable by DSC, whereas in this case, the specific heat change of both transitions is very similar.

For a better understanding of the nature of this intermediate transition, we examined several aspects of its behavior:

1. No connection between the presence or absence of T_i and the presence or absence of crystallinity in the material was found. In fact, Figure 5 shows the same material in an amorphous state, with and without T_i, and in a semicrystalline state, with and without T_i.
2. The presence or absence of T_i depends on the rate used to cool the polymer from the melt state. Figure 6 shows the "DSC standard scan" of the same material, in which T_i is present after polymerization, subjected to thermal treatments "B," "C," "D," and "E" given in the same figure: The samples were all taken to 250°C (a temperature higher than the melting point), allowed to stand for 5 min, and then cooled to −100°C at different constant cooling rates. Only in the case of the sample quenched in liquid nitrogen from 250°C (thermal history "E") did the intermediate transition not disappear.
3. T_i can be eliminated by heating the material to a temperature slightly above T_h. Figure 7 shows the "DSC standard scan" of several samples of the same material subjected to thermal treatments "F," "G," "H," "C," and "I": Samples were heated to different temperatures, between 120 and 270°C, kept at this temperature for 5 min, and then cooled at −5°C/min to −100°C. In all cases, T_i disappears. From Figures 6 and 7, it appears that thermal treatments have a great influence on T_i, but very little influence on T_h and T_s.
4. Some dynamic mechanical thermal analyses were carried out on compression-molded samples of Type VI polyurethane with a hard-to-soft-segment ratio of 80/20 to complement

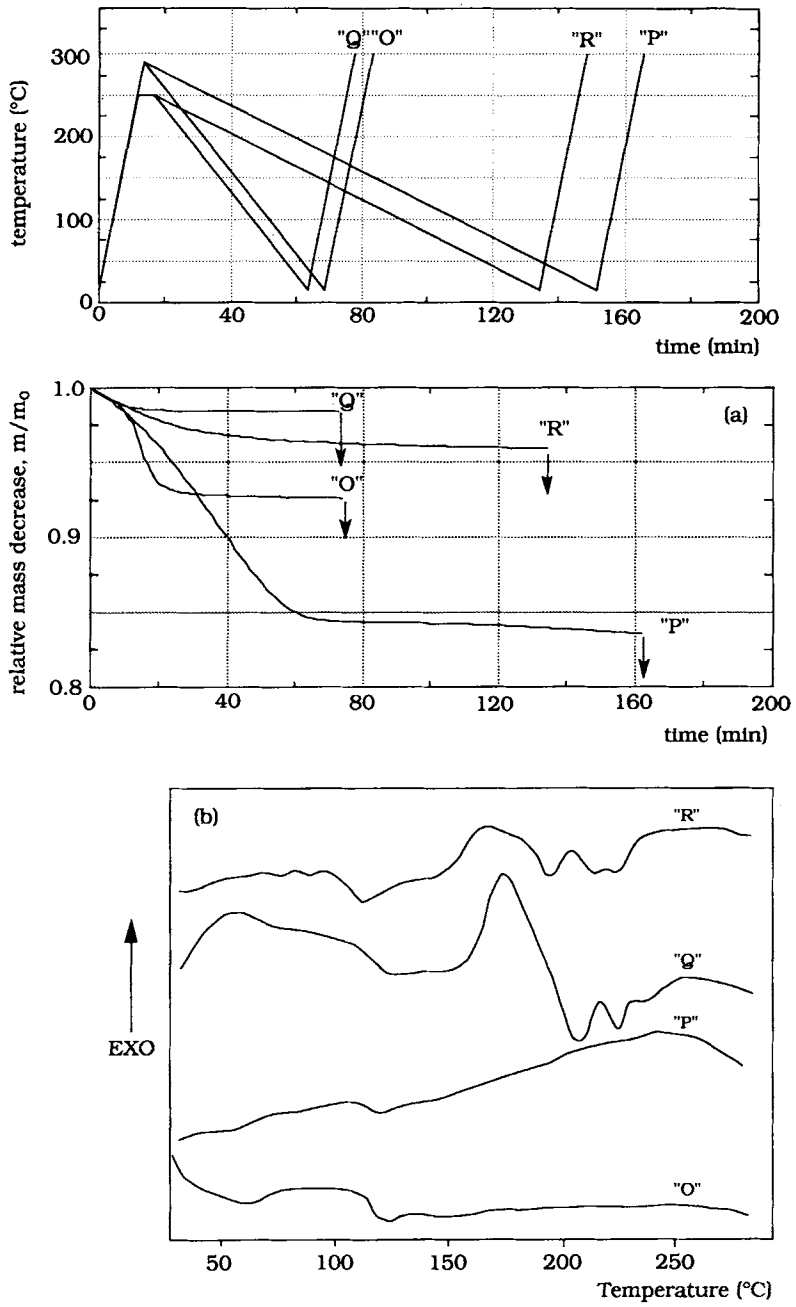

Figure 11 (a) Relative mass loss as a function of time for 90/10 : I : 110 polyurethane obtained by TGA during thermal cycles "O," "P," "Q," and "R" (also outlined at the top of the figure). (b) DTA curves for 90/10 : I : 110 polyurethane obtained during the last step of thermal cycles "O," "P," "Q," and "R."

the observations made on T_i from the DSC analysis.

Figure 8(a) gives tan δ results obtained from these measurements. The sample tested just after molding (curve 1) shows two peaks at −65 and 108°C and a shoulder at 50°C; the same material, after being thermally treated for 5 h at 120°C and then cooled to room temperature at a rate of −10°C/min (curve 2), shows that the peak at −65°C remains unchanged and the higher peak shifts to about 130°C, and the shoulder, to −10°C. Figure 8(b) shows the

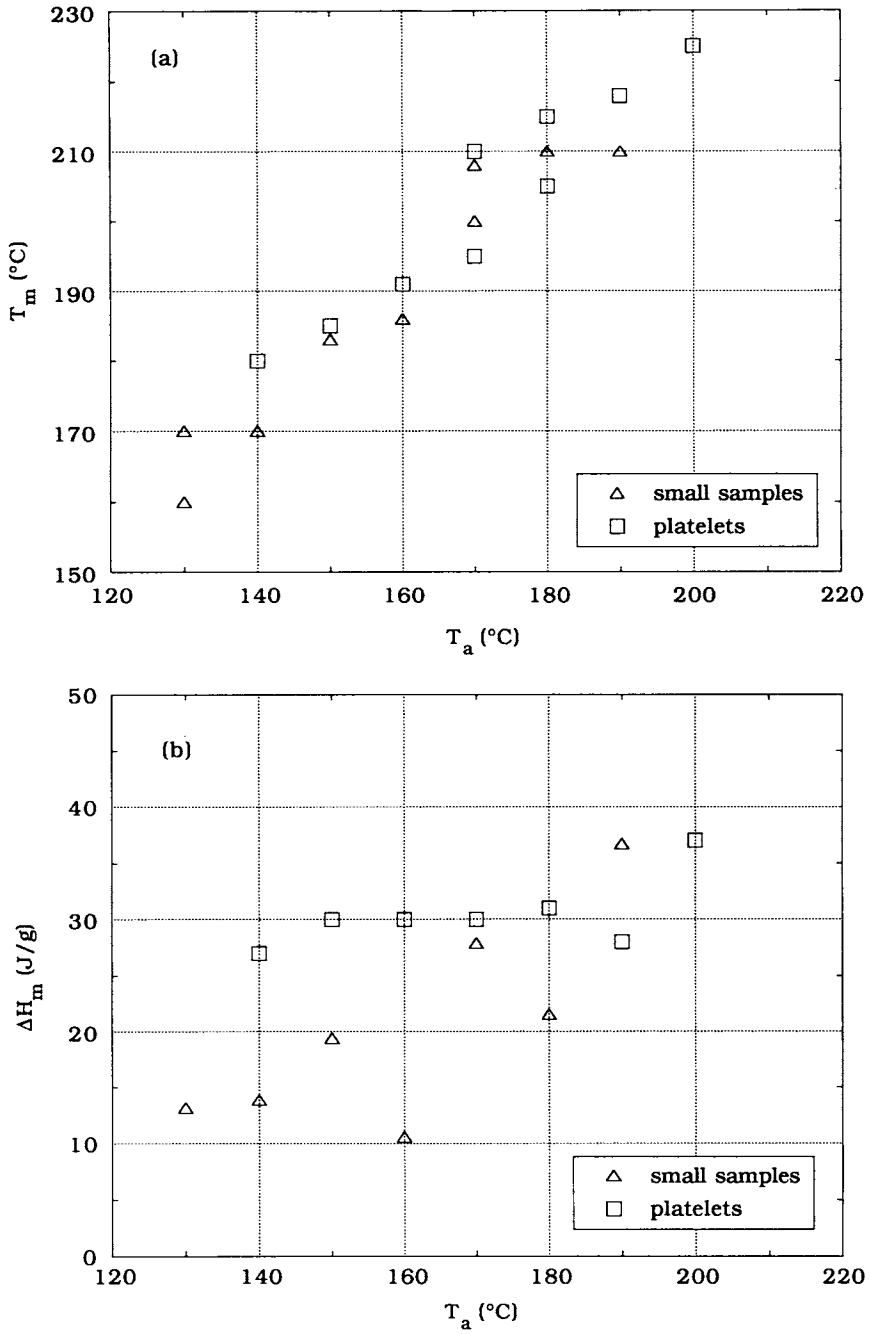

Figure 12 (a) Melting temperature, T_m, and (b) heat of fusion, ΔH, as a function of annealing temperature for 80/20 : II : 250 polyurethane.

DSC standard scan of the samples in Figure 8(a). Although some crystallinity is present, the amorphous phase shows transitions similar to those observed from tan δ.

From these dynamic mechanical tests, it would seem that the transition T_i observed in DSC corresponds to a viscoelastic relaxation, which appears to be dependent on thermal history.

3.5.2. Analysis of the Influence of Thermal Treatments on the Crystalline Phase

Nonisothermal Treatments. A 90/10 : I : 110 polyurethane, which showed its highest melting temperature at 218°C [Fig 1(c) and Table II], was subjected to several thermal treatments ("A," "J," "K," and "L") consisting of heating the material at

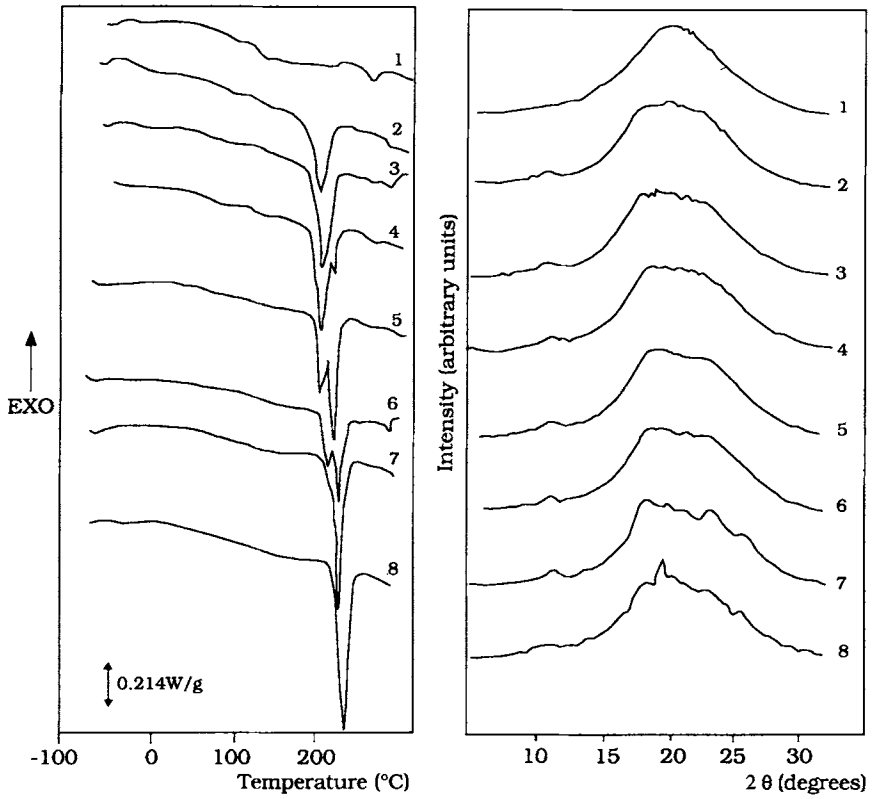

Figure 13 (a) DSC standard scans and (b) WAXS patterns of 80/20 : II : 250 polyurethane platelets after different annealings (see Table III).

a rate of 20°C/min to 290°C and then cooling it at different rates of between −2°C/min and −20°C/min. The DSC standard scans of these samples are shown in Figure 9. The following observations may be made:

1. The cooling rate of −5°C/min leads to completely amorphous materials.

Table III DSC Data for Polyurethane 80/20 : II : 250 Platelets Annealed at Different Temperatures

Sample No.	Annealing Temperature (°C)	T_m (°C)	ΔH_m (°C)
1	No treatment	—	—
2	140	180	27
3	150	185	30
4	160	191	30
5	170	195–210	30
6	180	205–215	31
7	190	218	28
8	200	225	37

2. Contrary to expectation, however, the higher cooling rates (−10°C/min and −20°C/min) produced crystalline materials or materials that crystallize during heating in the DSC. This apparently contradictory result may be explained by the fact that, with high cooling rates, the material does not remain above its melting point long enough to destroy the crystalline domains completely.

With the aim of clarifying this aspect, two additional thermal treatments, "N" and "M," were carried out. In thermal history "M," the sample is maintained at 250°C during 20 min and then cooled at −20°C/min, whereas in history "N," the sample is kept at 290°C for 10 min and then cooled to 20°C. The thermal treatments, together with the "DSC standard scan" of the treated materials, are shown in Figure 10: Only thermal history "N" is capable of destroying the crystallinity completely and gives an amorphous material; further, for this material, although from the DSC scan melting seemed complete at 250°C [Fig. 1(c)], even a long stay at this temper-

ature is not sufficient to completely eliminate crystalline nuclei.

3. The DSC curve in Figure 9, corresponding to the −2°C/min cooling rate (thermal history "J"), exhibits an exothermic peak in the high-temperature zone of the thermogram that is probably due to thermal degradation.[33] To investigate this possibility, thermogravimetric analysis (TGA) was conducted on some samples of the polyurethane 90/10 : I : 110 subjected to different thermal treatments.

Results of this analysis are shown in Figure 11, which reports, together with the thermal histories applied to the samples, the mass decrease [Fig. 11(a)] and the results of DTA [Fig. 11(b)] performed during the last step in the thermal history (heating from 15 to 300°C at 20°C/min). From these results, we may conclude that

- Consistently with previous observations, for the treatments that take the sample to 290°C and then cool it at −2°C/min or −5°C/min, the crystallinity disappears [see curves "O" and "P" of Fig. 11(b)], while 5 min at 250°C, followed by cooling at −2°C/min or −5°C/min, is not sufficient to destroy the crystallinity; in fact, the material crystallizes during the third step of the thermal treatment [see curves "Q" and "R" in Fig. 11(b)].
- The sample cooled at the lowest rate (−2°C/min; history "P") shows again an exothermic peak during the last scan after the treatment at high temperature. If we analyze the TGA results [Fig. 11(a)], this sample exhibited the greatest weight loss, thus confirming the degradation assumption.

Isothermal Treatments. The influence of isothermal treatments on phase structure was studied on an 80/20 : II : 250 polyurethane, which is amorphous after polymerization (see Table II). Some experiments were conducted on small samples (about 15 mg) in the DSC. Each sample was annealed at a constant temperature between 120 and 190°C for 2 h and then rapidly cooled to room temperature. Crystallinity was effectively induced by annealings above 130°C. A well-defined trend was found for melting temperatures as a function of annealing temperature. Figure 12(a) shows that T_m (the temperature of the highest endothermic peak from DSC

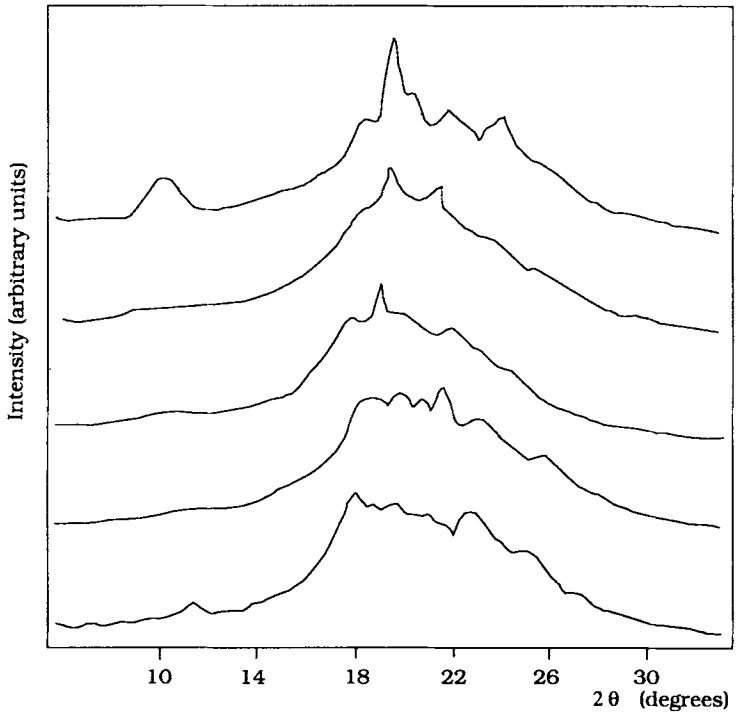

Figure 14 WAXS patterns of samples of 80/20 : II : 250 polyurethane subjected to specific thermal histories to bring out the presence of different crystalline forms.

curves) increases with the annealing temperature, reaching a fairly constant value of about 210°C for annealing temperatures above 180°C.

The heat of fusion, ΔH_m, which we have used previously as a measure of crystallinity, showed, in spite of some data scatter, a contemporaneous increase with annealing temperature [Fig. 12(b)]. To further investigate the effect of isothermal treatments on crystallinity, thermal annealings were also carried out on platelets suitably prepared, so that WAXS analysis can be performed on them. Thermal treatments lasted 24 h to avoid crystallinity profiles.

DSC scans and diffraction patterns of these platelets are shown in Figure 13 and their analysis in Table III. Although it may be noted that multiple peaks are more evident for the larger samples treated for 24 h [Fig. 13(a)], as can be observed in Figure 12(a) and (b), in which data obtained from these platelets are also given, T_m and ΔH_m for both types of samples show very similar trends.

WAXS results [Fig. 13(b)] show that increase in the annealing temperature gives rise to a change in the diffraction peaks, with some tendency toward ordering, deduced from the change in the shape of the curves. The untreated sample displays a diffuse scattering maximum for 2Θ from 12° to 30°, suggesting a substantially amorphous morphology, and weak diffraction peaks displayed by the samples annealed at intermediate temperatures become distinct diffraction peaks for samples annealed at 190 and 200°C.

These diffraction patterns also revealed that the relative intensity of the peaks observed for treatments at 190 and 200°C is not the same. This finding agrees with previous statements[11,28,33] and suggests the possible existence of more than one crystalline form. Extra evidence of this fact can be seen in Figure 14, which shows diffraction patterns of different samples of 80/20 : II : 250 polyurethane, which underwent specific thermal treatments so as to bring out the differences in the relative intensity of the principal peaks.

Figure 15 shows the amorphous index calculated from the curves shown in Figure 13(b). The amorphous index was chosen to avoid having to distinguish between the contributions to crystallinity of each crystalline form. It appears that the amorphous index decreases with the increase in annealing temperature, thus indicating that increasing the annealing temperature, at least within the temperature range examined, enhances the structural arrangement of the hard segments promoting crystallization.

4. CONCLUSIONS

In this first work, we examined the possibility of making rigid toughened polyurethanes and have analyzed the polymerization variables and the phase structure of the resulting polymers. The results from the present study show the following:

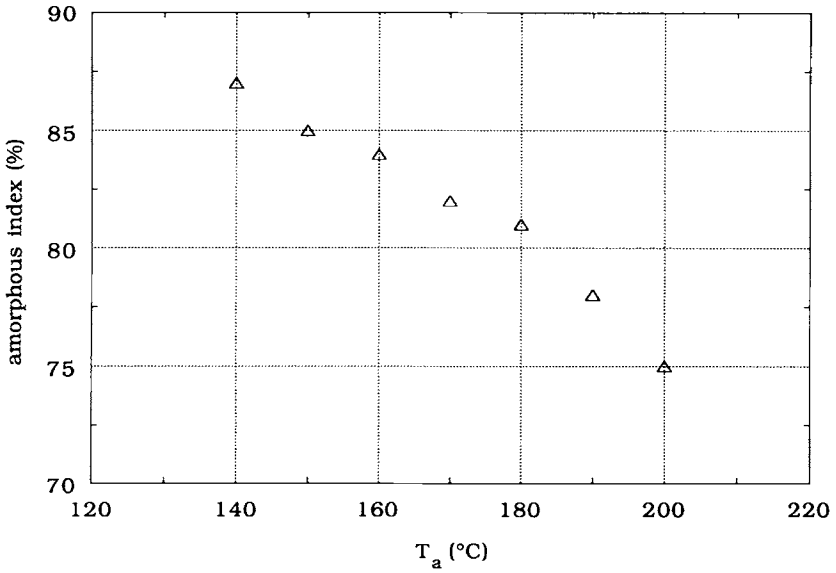

Figure 15 Amorphous index as a function of annealing temperature for 80/20 : II : 250 polyurethane.

1. These rigid polyurethanes, despite their thermoplastic characteristics, appear to be insoluble at room temperature in the solvents normally used for elastomeric polyurethanes, probably due to the presence of cross-linking sites in very low concentration, not detectable by IR analysis, resulting from secondary reactions or to the presence of strong hydrogen bonding in the hard domains.
2. Structure of both the crystalline and the amorphous phase of these polyurethanes have turned out to be very complex and strongly dependent on the thermal history undergone during polymerization, as well as on further thermal treatments.
3. Three second-order transitions of the same order of magnitude and detectable by DSC were observed. The lowest one corresponds to the glass transition of the soft segments, whereas the intermediate and highest ones seem to correspond to transitions of the hard phase. Our results are consistent with Brunette et al.'s[29] statements suggesting the existence of a bimodal length distribution of the hard segments, giving rise to thermally activated rearrangements of the amorphous hard phase.
4. A comparison of six polyurethane types, differing basically on the chain extenders, indicates that every polyurethane type studied can be either amorphous or semicrystalline, depending on the hard/soft-segment ratio and on the polymerization conditions chosen. Type VI, based on butanediol and 1-phenyl-1,2-ethanediol (molar ratio 4/1), leads to polymers with the lowest tendency to crystallize, even though a formulation producing only amorphous products could not be found.
5. The premature crystallization of oligomeric materials during polymerization hinders further polymerization. "Curing temperatures" above crystallization temperatures produce amorphous polyurethanes with a high degree of polymerization.
6. Crystallinity of amorphous samples may be induced by annealing. WAXS analysis of the 80/20 : II : 250 polyurethane suggests that more than one crystalline form is present.

We thank Dr. G. F. Lunardon (Montedipe S.p.A., Porto Marghera) for helpful discussions and for providing us with some of the raw chemicals; Prof. M. Zocchi (Brescia University) for invaluable assistance in the WAXS measurements and their interpretation, and Prof. M. Pizzoli (Bologna University) for carrying out the DTMA measurements. One of the authors (P. M. F.) would also like to thank CONICET (National Research Council, Argentina) and Fundación Antorchas for fellowship support throughout this work.

REFERENCES

1. R. Bonart, *J. Macromol. Sci. Rev. Macromol. Chem.*, **C4**(2), 313 (1970).
2. S. L. Cooper and A. V. Tobolsky, *J. Appl. Polym. Sci.*, **10,** 1837 (1966).
3. C. H. Y. Chen-Tsai, E. L. Thomas, W. J. Macknight, and N. S. Schneider, *Polymer,* **27,** 659 (1987).
4. C. H. Y. Chen, R. M. Briber, E. L. Thomas, M. Xu, and W. J. Macknight, *Polymer,* **24,** 1333 (1983).
5. A. L. Chang, R. M. Briber, E. L. Thomas, R. J. Zdrahala, and F. E. Critchfield, *Polymer,* **23,** 1060 (1982).
6. J. T. Koberstein and R. S. Stein, *Polymer,* **25,** 171 (1984).
7. T. K. Kwei, *J. Appl. Polym. Sci.,* **27,** 2891 (1982).
8. L. M. Leung and J. T. Koberstein, *Macromolecules,* **19,** 706 (1986).
9. R. M. Briber and E. L. Thomas, *J. Polym. Sci. Polym. Phys. Ed.,* **23,** 1915 (1985).
10. J. Blackwell, J. R. Quay, and M. R. Nagarajan, *J. Polym. Sci. Polym. Phys. Ed.,* **22,** 1247 (1984).
11. J. Blackwell and C. D. Lee, in *Advances in Urethane Science and Technology,* K. C. Frisch, and D. Klempner, Eds., Technomic, Lancaster, PA, 1984, Vol. 9, pp. 25–46.
12. R. E. Camargo, C. W. Macosko, M. Tirrell, and S. T. Wellinghoff, *Polymer,* **26,** 1145 (1985).
13. S. Abouzahr, G. L. Wilkes, and Z. Ophir, *Polymer,* **23,** 1077 (1982).
14. S. Abouzahr and G. L. Wilkes, *J. Appl. Polym. Sci.,* **29,** 2695 (1984).
15. I. D. Fridman, E. L. Thomas, L. J. Lee, and C. W. Macosko, *Polymer,* **21,** 393 (1980).
16. G. F. Lunardon, *Atti IIIa Giornata Chim. Montedison Milano,* **22,** 1 (1985).
17. D. J. Goldwasser and K. Onder, U.S. 4,376,834 (Cl. 521-159; C08G18/14), (March 15, 1983), Appl. 311,198 (Oct. 14, 1981).
18. M. Serrano, W. J. Macknight, E. L. Thomas, and J. M. Ottino, *Polymer,* **28,** 1667 (1987).
19. R. Von Merten, D. Laurerer, G. Braun, and M. Dalm, *Macromol. Chem.,* **101,** 337 (1967).
20. J. E. Spruiell and E. S. Clark, in *Methods of Experimental Physics,* R. A. Fava, Ed., Vol. 16, Part B, Academic Press, New York, 1980, p. 118.
21. C. G. J. Seefried, J. V. Koleske, F. E. Critchfield, and C. R. Pfaffenberger, *J. Polym. Sci. Polym. Phys. Ed.,* **18,** 817 (1980).

22. M. Xu, W. J. Macknight, C. H. Y. Chen, and E. L. Thomas, *Polymer,* **24,** 1327 (1983).
23. C. H. Y. Chen-Tsai, E. L. Thomas, W. J. Macknight, and N. S. Schneider, *Polymer,* **27,** 659 (1986).
24. W. P. Yang, C. W. Macosko, and S. T. Wellinghoff, *Polymer,* **27,** 1235 (1986).
25. C. S. Schollenberger and K. Dinbergs, *J. Polym. Sci. Polym. Symp.,* **64,** 351 (1978).
26. K. K. S. Hwang, G. Wu, S. Burn Lin, and S. L. Cooper, *J. Polym. Sci. Polym. Chem. Ed.,* **22,** 1677 (1984).
27. T. A. Speckhard, V. S. C. Chang, and J. P. Kennedy, *Polymer,* **26,** 55 (1985).
28. R. Russo and E. L. Thomas, *J. Macromol. Sci.-Phys. B,* **22**(4), 553 (1983).
29. C. M. Brunette, S. L. Hsu, M. Rossman, W. J. Macknight, and N. S. Schneider, *Polym. Eng. Sci.,* **21**(11), 668 (1981).
30. L. Curvé, J. P. Pascault, G. Boiteux, and G. Seytre, *Polymer,* **32**(2), 343 (1991).
31. G. Lunardon, Y. Sumida, and O. Vogl, *Angew. Macromol. Chem.,* **87,** 1313 (1980).
32. B. Bengston, C. Feger, W. J. Macknight, and N. S. Schneider, *Polymer,* **26,** 895 (1985).
33. L. M. Leung and J. T. Koberstein, *Macromolecules,* **19,** 706 (1986).

Received June 10, 1992
Accepted September 29, 1992